

1 **Lysophosphatidylcholine induces oxidative stress in human endothelial**
2 **cells via NOX5 activation - implications in atherosclerosis**

3

4 Josiane Fernandes da Silva¹, Juliano V Alves¹, Julio Neto¹, Rafael M Costa¹,
5 Karla B Neves², Rheure Lopes², Livia Carmargo², Francisco Rios², Augusto
6 Montezano², Rhian M Touyz², Rita C Tostes¹.

7

8 ¹Pharmacology Department, Ribeirao Preto Medical School, University of Sao
9 Paulo (FMRP-USP)– USP, Brazil.

10 ²Institute of Cardiovascular and Medical Sciences, BHF Glasgow
11 Cardiovascular Centre, University of Glasgow, Glasgow, UK.

12

13 * Corresponding Author:

14

15 Rita C Tostes

16 Dept. of Pharmacology

17 Ribeirao Preto Medical School

18 University of Sao Paulo

19 Av Bandeirantes 3900

20 Ribeirao Preto - SP 14049-900

21 Brazil

22 Phone: +55 16 3315-4529 / 3315-3181

23 rtostes@usp.br

24

25 **Abstract**

26 **Introduction:** NOX5 belongs to the nicotinamide adenine dinucleotide
27 phosphate (NADPH) oxidases (NOX) family, and its vascular expression and
28 activity are up regulated in cardiovascular diseases, such as hypertension and
29 atherosclerosis. Although NOXes are activated by many factors that contribute
30 to formation and progression of atherosclerotic lesions, including lipids and
31 oxidized low-density lipoprotein (oxLDL), mechanisms involved in NOX5
32 activation in atherosclerotic processes are still unclear. This study tested the
33 hypothesis that lysophosphatidylcholine (LPC), a proatherogenic component of
34 oxLDL, induces endothelial calcium influx, which drives NOX5-dependent
35 reactive oxygen species (ROS) production, oxidative stress and endothelial cell
36 dysfunction. **Methods:** Human aortic endothelial cells (HAEC) were stimulated
37 with LPC (10^{-5} M, for different time points). Pharmacological inhibition of NOX5
38 (Melittin, 10^{-7} M) and NOX5 gene silencing (siRNA) were used to determine the
39 role of NOX5-dependent ROS production in endothelial oxidative stress induced
40 by LPC. ROS production was determined by lucigenin assay and electron
41 paramagnetic spectroscopy (EPR), calcium transients by Fluo4 fluorimetry and
42 NOX5 activity and protein expression by pharmacological assays and
43 immunoblotting, respectively. **Results and Discussion:** LPC increased ROS
44 generation in endothelial cells at both short (15 min) and long (4 h) stimulation
45 times. LPC-induced ROS at both 15 min and 4 h was abrogated by a selective
46 NOX5 inhibitor and by knockdown of NOX5 expression. NOX1/4 dual inhibition
47 and selective NOX1 inhibition only decreased ROS generation at 4 h. LPC
48 increased HAEC intracellular calcium, important for NOX5 activation, and this
49 was blocked by nifedipine and thapsigargin. Bapta-AM and EGTA, selective

50 Ca²⁺ chelators, prevented LPC-induced ROS production. NOX5 knockdown
51 decreased LPC-induced ICAM-1 mRNA expression and monocyte adhesion to
52 endothelial cells.

53 **Conclusion:** These results suggest that NOX5, by mechanisms linked to
54 increased intracellular calcium, is key to early LPC-induced endothelial
55 oxidative stress and pro-inflammatory processes. Since these are important
56 events in the formation and progression of atherosclerotic lesions, this study
57 highlights an important role for NOX5 in atherosclerosis.

58

59

60 **Introduction**

61 Atherosclerosis remains a significant cause of morbidity and mortality
62 worldwide, predisposing individuals to thrombosis, stroke, and other
63 cardiovascular diseases (CVD) [1]. In the last decades, the advance in
64 atherosclerosis knowledge has been remarkable. However, mechanisms
65 involved in atherosclerotic plaque formation need further clarification in many
66 aspects, including the role of NOX-induced oxidative stress [1].

67 The formation and progression of atherosclerotic lesions are directly related to
68 oxidative stress in the vascular wall. Excessive reactive oxygen species (ROS)
69 production is associated with endothelial dysfunction, lipids accumulation,
70 apoptosis, inflammatory cytokines and monocyte recruitment [1, 2]. In all these
71 processes, increased nicotinamide adenine dinucleotide phosphate (NADPH)
72 oxidases (NOX) activity is key to increase superoxide anion (O_2^-) generation,
73 which results in oxidative stress and more severe vascular lesions [1].

74 Four NOX isotypes are expressed in human endothelial cells, NOX1, NOX2,
75 NOX4, and NOX5 [3]. These enzymes belong to a family of proteins that
76 catalyze O_2 reduction to produce O_2^- , using NADPH as the electron donor
77 ($NADPH + 2O_2 \rightarrow NADP^+ + H^+ + 2O_2^-$). NOX1, NOX2 and NOX4 require
78 phox22 and other protein subunits, such as NOXOA1, phox67, and phox47 to
79 function [3]. Unlike other NOX isoforms, NOX5 does not require modulatory
80 subunits for its activation. The activity of this NOX isotype depends on gene
81 expression, subcellular localization, post-translational changes, and cytoplasmic
82 Ca^{2+} concentration ($[Ca^{2+}]_i$). In endothelial cells, knockdown of NOX5
83 attenuates PCNA and VCAM expression induced by angiotensin II [4],
84 suggesting that NOX5 plays a role in endothelial proliferation and monocyte

85 recruitment. Moreover, NOX5 expression is increased in patients with coronary
86 artery diseases and associated with atherosclerosis severity [5]. However,
87 mechanisms that induce NOX5 expression and activity in atherosclerosis
88 remain to be elucidated.

89 Lysophosphatidylcholines (LPCs) are a group of bioactive lipids involved in the
90 pathogenesis of atherosclerosis [6, 7]. LPC is a proatherogenic component of
91 oxidized low-density lipoprotein (oxLDL) [8, 9] that activates pro-inflammatory
92 and pro-oxidative cellular responses [10, 11, 12]. In humans, some LPC species
93 are associated with atherosclerotic plaque [13, 14], and atheroma plaques from
94 diabetic patients are significantly enriched with 2-arachidonoyl-
95 lysophosphatidylcholine [15]. Furthermore, LPC induces endothelial cell
96 activation through Ca^{2+} -dependent signaling [12] and mitochondrial ROS
97 production [16]. However, it is not clear whether NOX5 contributes to LPC-
98 induced endothelial oxidative stress.

99 Therefore, this study's premise is that LPC stimulates NOX5 activity, which
100 contributes to oxidative stress and endothelial dysfunction associated with
101 atherosclerotic processes.

102

103

104 **Material and Methods**

105 **Cell culture**

106 To assess whether NOX5 contributes to LPC-induced ROS production,
107 primary cultured, low passage (p5-p7), aortic endothelial cells (HAEC, ATCC®,
108 Middlesex, UK; PCS-100-011) were used. HAEC were cultured in endothelial
109 cell growth medium (Promocell®) supplemented with penicillin/streptomycin
110 (50 µg/mL) and endothelial cell growth medium supplement (10 mL,
111 Promocell®). Before stimulation protocols, confluent cells were made quiescent
112 by incubation for two hours (h) in low-serum medium (0.5% fetal bovine serum,
113 FBS). For the mechanistic studies, drugs and their respective concentrations
114 were as follows: Lysophosphatidylcholine (Sigma-Aldrich, cat. Number: L-4129,
115 10⁻⁵ M, [17]); Tiron (ROS scavenger, Sigma-Aldrich, cat number:172553, 10⁻⁴ M,
116 [18]); GKT137831 (NOX1/4 inhibitor, Cayman chemical, 10⁻⁵ M, [19]); NoxA1ds
117 (NOX1 inhibitor, Tocris, 10⁻⁵ M, [19]); Melittin (NOX5 inhibitor, 10⁻⁷ M, [20]);
118 Nifedipine (L-type calcium channel blocker, Tocris, 10⁻⁸ M, [21]); Thapsigargin
119 (SERCA ATPase inhibitor, Tocris, 10⁻⁷ M, [22]), Ionomycin (Calcium ionophore,
120 Tocris, 10⁻⁶ M, [23]), Bapta-AM (membrane-permeant selective Ca²⁺ chelator,
121 Invitrogen, 5 x 10⁻⁶ M, [24], EGTA (Ca²⁺ chelator, Sigma-Aldrich, 2 x 10⁻³ M,
122 [25]). Cells were incubated with the inhibitors, in individual protocols, for 30
123 minutes (min) before the stimulation with LPC. The inhibitors were kept during
124 the stimulation with LPC.

125

126 **ROS measurement by Chemiluminescence assay**

127 LPC-induced ROS generation was assessed by chemiluminescence with
128 NADPH as the substrate and lucigenin as the electron acceptor [26].

129 Endothelial cells were stimulated with LPC (10^{-5} M) for various time intervals: 5
130 min, 15 min, 30 min, 1 h, 4 h, 8 h, and 24 h. The two highest ROS production
131 stimulation times were chosen to study LPC's mechanisms leading to ROS
132 generation. In some experiments, cells were pre-incubated for 30 min with
133 inhibitors, as described above. After stimulation, cells were washed with PBS
134 and harvested in 100 μ L lysis buffer [2×10^{-2} M KH_2PO_4 ; 10^{-3} M EGTA, and
135 protease inhibitors: 1 μ g/ml of aprotinin, 1 μ g/ml of leupeptin, 1 μ g/ml of
136 pepstatin, and 10^{-3} M phenylmethylsulfonyl fluoride (PMSF)]. 50 μ L of the
137 sample were added to 175 μ L assay buffer [5×10^{-2} M KH_2PO_4 , 10^{-3} M EGTA,
138 1.5×10^{-3} M sucrose, and 5×10^{-6} M lucigenin (98% purity, Sigma)]. Then, the
139 first reading was performed and considered as basal reading. NADPH (98%
140 purity, 10^{-4} M; Sigma) was added to each sample, and the luminescence signal
141 was measured, for 30 cycles of 18 seconds each, in a luminometer (Lumistar
142 Galaxy, BMG Lab Technologies, Germany). Basal and blank buffer readings
143 were subtracted from the respective samples reading. Results are expressed
144 as a percentage of control values (% of control) of the relative light units (RLU)
145 per protein content, as measured by the BCA assay (Thermo Fisher, 23225).

146

147 **Superoxide anion (O_2^-) quantification by Electron Paramagnetic**

148 **Resonance (EPR) spectroscopy**

149 The cell-permeable spin-trapping probe, CMH (1-hydroxy-3-methoxycarbonyl-
150 2,2,5,5-tetramethylpyrrolidine; Enzo life science, UK; cat. ALX430117), was
151 used to detect intracellular superoxide anion in HAEC by EPR spectroscopy
152 [27, 28]. After each experimental condition, cells were washed with sterile PBS
153 and incubated in Krebs/Hepes buffer (pH= 7.35) containing 0.5 mM CMH, 5 μ M

154 DETC, 25 μ M deferoxamine for 30 min in a CO₂ incubator at 37°C. The solution
155 was removed, and 100 μ L of Krebs/Hepes buffer without CMH was added and
156 then, cells were gently and quickly scraped. Approximately 50 μ L were
157 transferred into a capillary glass tube (Noxygen Science Transfer &Diagnostics)
158 and placed inside the E-scan spectrometer's cavity for reading. The remaining
159 sample volume was used for total protein determination by the BCA method
160 (Pierce™ BCA Protein Assay Kit, Thermo Fisher Scientific, cat. 23225). The
161 results are expressed as a percentage of the control condition, spectrum
162 amplitude value (in arbitrary units) per protein concentration. Acquisition
163 spectrometer (Bruker® Biospin Corp.) parameters were microwave power
164 21.98mV; microwave frequency 9.463GHz; number of scans 30; sweep width
165 50G; modulation amplitude 2G; conversion time, 656 ms; time constant, 656
166 ms; resolution, 512 points and receiver gain 1×10^5 . The sample temperature
167 was kept at 21°C by the Temperature & Gas Controller unit, connected to the
168 spectrometer. Spectra were analyzed by using Win EPR software, supplied by
169 Bruker Corp.

170

171 **Immunoblotting**

172 Quiescent HAECs were stimulated with LPC 10^{-5} M for 15 min or 4 h, in
173 the presence of vehicle or different inhibitors at 37°C. After stimulation, cells
174 were quickly washed in ice-cold PBS, and protein extraction was performed in
175 lysis buffer [50 mmol/L Tris-HCl (pH 7.4) containing 1% Nonited P-40, 0.5%
176 sodium deoxycholate, 150 mmol/L NaCl, 1 mmol/L EDTA, 0.1% sodium dodecyl
177 sulfate (SDS), 1 mmol/L phenylmethylsulfonyl fluoride (PMSF), 1 μ g/mL
178 pepstatin A, 1 μ g/mL leupeptin and 1 μ g/mL aprotinin]. Then, the lysate was

179 sonicated and cleared by centrifugation at 10,000 rpm for 10 min. Protein
180 concentration was assessed by the BCA method (Pierce™ BCA Protein Assay
181 Kit, Thermo Fisher Scientific, cat. 23225). 30 ug protein were separated by
182 electrophoresis on 10% SDS polyacrylamide gel and transferred to a
183 nitrocellulose membrane. Membranes were blocked with Tris-buffered solution
184 (TBS) containing 5% skim milk and 0.01 % Tween for 1 h at room temperature.
185 Then, membranes were incubated with specific primaries antibodies overnight
186 at 4°C, and secondaries antibodies for 1 hour at room temperature. Primary
187 and secondary antibodies used in Western blot assays were as follows: rabbit
188 anti-NOX5 (Abcam / ab191010 / 1:1000); β -actin (Cell Signaling Technology / #
189 4967 / 1:3000); peroxidase (HRP)-conjugated-anti-Rabbit IgG (Sigma / A0545 /
190 1:7500). Immunocomplexes were detected by chemiluminescence reaction
191 (Luminata Forte HRP Substrate; Millipore, USA), and densitometric analysis
192 was performed with ImageQuant 1.3 software. Protein expression levels were
193 normalized to the internal housekeeping protein (β -actin).

194

195 **Quantitative PCR (qPCR)**

196 mRNA expression of NADPH oxidase 5 (NOX5), intercellular adhesion
197 molecule 1 (ICAM1) and glyceraldehyde 3-phosphate dehydrogenase (GAPDH)
198 was quantified by qPCR in non-stimulated endothelial cells or LPC-stimulated
199 cells for 4 h or NOX5-silenced LPC-stimulated cells. Briefly, TRIzol® Reagent
200 (Invitrogen) was used to extract total RNA from cells. RNA was treated with
201 RNase-free DNase I, and 2 μ g of RNA was used in reverse transcriptase
202 reactions, following the manufacturer's instruction (High capacity cDNA, Applied
203 Biosystems #4368813). TaqMan Fast Advanced Master Mix (Applied

204 Biosystems, # 4444557) was used to perform real-time PCR amplification. The
205 relative mRNA expression (target gene/ housekeeping gene) was calculated by
206 the $2^{-\Delta\Delta CT}$ method. The assay primers used are as follows: h_NOX5
207 (Hs00225846_m1); h_ICAM-1, (Hs00164932_m1); h_GAPDH
208 (Hs02786624_g1), from Thermo Fisher Scientific.

209

210 **Calcium influx measurement**

211 Calcium signal was assessed by dye Fluo-4 fluorescence (Invitrogen,
212 F14201). After a 45-minute incubation period with the inhibitors, cells were
213 quickly washed in Phosphate-buffered saline (PBS) and DMEM solution,
214 without phenol and with Fluo-4 AM (2 μ M), was added, for 30 min at 37° C, to
215 load the cells. Following incubation, cells were washed and incubated with the
216 medium for 20 min at 37°C. Fluorescence-based measurements of Ca²⁺ were
217 performed using a fluorimeter plate reader (FlexStation 3 system, Molecular
218 Devices, San Jose, CA, USA). The software was set to acquire five basal
219 readings with an interval of 30 seconds (s). LPC solution (10⁻⁵ M, final
220 concentration) was added to cells and readings were recorded every 90 s, for
221 20 min. The excitation/emission wavelengths for the Fluo-4 signal recordings
222 were 495 / 505 nm, respectively, and values were normalized to the basal value
223 recording. LPC-induced extracellular calcium influx was evaluated in cells pre-
224 incubated with nifedipine (L-type calcium channel blocker, Tocris, 10⁻⁸ M).
225 Additionally, the role of intracellular endoplasmic reticulum calcium stocks in the
226 LPC effects was estimated in cells pretreated with thapsigargin (SERCA
227 ATPase inhibitor, Tocris, 10⁻⁷ M). Cells treated with ionomycin (Calcium
228 ionophore, Tocris, 10⁻⁶ M) were used as a positive control. The results were

229 expressed as intensity of the signal (F)/ basal signal (F₀) mean (RFU, relative
230 fluorescence units) or area under the curve (AUC) of the fluorescence signal.

231

232 **NOX5 Silencing**

233 NOX5 downregulation was performed in HAEC using NOX5 siRNA (ID
234 s35770, Silencer® Select siRNA, Thermo Fischer Scientific) complexed with
235 Lipofectamine™ RNAiMAX (Thermo Fischer Scientific) as transfection reagent
236 in Opti-MEM (GIBCO™) without serum or antibiotics for 24 h. A non-targeting
237 negative control siRNA with the same chemical modifications (Silencer® Select
238 Negative Control No. 1 siRNA, Invitrogen) was used as control siRNA. NOX5
239 protein expression was performed to confirm downregulation of NOX5
240 expression.

241

242 **Monocyte attachment assay**

243 To evaluate whether NOX5 contributes to monocytes adhesion on
244 endothelial cells, NOX5-silenced endothelial cells were stimulated with LPC and
245 exposed to fluorescence-labeled monocytes. The adhered cells were estimated
246 by the fluorescence signal [29, 30]. Briefly, HAEC were cultured in 24-well
247 plates, and NOX5 silencing was performed as described above. Then, the cells
248 were stimulated with LPC 10⁻⁵ M for 4 h. Monocytes obtained from the
249 American Type Culture Collection (THP-1) were cultured in RPMI medium
250 supplemented with penicillin/streptomycin and 10% FBS. THP-1 were washed
251 and incubated in saline solution containing 0.1% bovine serum albumin and 10⁻⁶
252 M of CellTrace CFSE Cell Proliferation (Life Technologies), a fluorescent probe,
253 for 20 min at 37°C. After the stimulation period, HAEC were washed twice in

254 PBS and incubated with labeled monocytes (2×10^5 cells/mL) for 30 min at 37°C
255 in 5% CO₂ to allow adhesion. At the end of this step, non-adherent monocytes
256 were removed by gently washing with PBS, and the cells were de-attached with
257 trypsin and transferred to an opaque plate. Images from the labeled monocytes
258 were captured in a fluorescence microscope (Leica DMI inverted microscope)
259 and the fluorescence signal was acquired with a fluorimeter plate reader
260 (FlexStation 3 system, Molecular Devices, San Jose, CA, USA). The
261 fluorescence signal estimated the number of adherent monocytes.

262

263 **Statistical analysis**

264 Statistical analysis of data was performed using GraphPad Prism 8.0
265 (GraphPad Software, San Diego, CA). Data are represented as mean \pm
266 standard error of the mean (SEM). Differences among the groups were
267 evaluated using Student's t-test or one-way ANOVA followed by Dunnett's or
268 Tukey post-test, when appropriated. $p < 0.05$ was considered statistically
269 significant.

270

271 **Results**

272 **LPC induces ROS production in HAEC cells**

273 To determine ROS generation induced by LPC, HAEC were stimulated
274 with LPC (10^{-5} M) for various times: 5 min, 15 min, 30 min, 1 h, 4 h, 8 h, and 24
275 h (figure 1). LPC induced ROS generation in endothelial cells (HAEC) in a time-
276 dependent manner (figure 1). ROS levels increased after 15 min and increased
277 up to 4 h after stimulation with LPC (10^{-5} M). After 4 h, ROS levels returned to
278 the basal condition (figure 1C). In the subsequent experimental protocols, LPC-
279 induced ROS generation was assessed at two time points: 15 min and 4 h.

280

281 **LPC-induced ROS production is prevented by NOX5 pharmacological**
282 **inhibition and by NOX5 siRNA silencing**

283 To determine whether LPC influences endothelial cell ROS generation
284 through NOX-dependent processes, cells were exposed to different NOX
285 isoform inhibitors. First, endothelial cells were pre-incubated with GKT137831
286 10^{-5} M, a NOX1/4 dual inhibitor. GKT137831 did not reduce LPC-induced ROS
287 generation at 15 min (figure 2A) but prevented ROS production at 4 h of LPC
288 stimulation (figure 2B), suggesting that NOX 1 and 4 do not participate in the
289 early stages of LPC-induced ROS generation. ROS generation in figure 2 was
290 determined by Lucigenin assay. Similar results were observed using EPR
291 spectroscopy (Supplementary figure 1).

292 Moreover, NOX 1 inhibition (nox1ds 10^{-5} M) attenuated ROS production
293 induced by LPC stimulation at 4 h (Supplementary figure 1D), but not at 15 min,
294 supporting that NOX1 participates in ROS production induced by LPC at later-
295 times.

296 Unlike GKT137831 and noxa1ds, Melittin (10^{-7} M), a NOX5
297 pharmacological inhibitor, blocked LPC-induced ROS generation at both early
298 and late stimulation time points (figure 3). ROS generation was determined
299 both by lucigenin assay (figures 3A and 3B) and EPR spectroscopy (figures 3C
300 and 3D).

301 Supporting data from the pharmacological assays, silencing of NOX5
302 expression (siRNA) attenuated LPC-induced ROS production in HAEC cells
303 (figure 4).

304

305 **LPC stimulates calcium influx**

306 An important mechanism for NOX5 activation is binding to intracellular
307 calcium. To determine whether LPC increases intracellular calcium
308 concentration at early time points of stimulation and whether this is linked to
309 NOX5-dependent ROS production, calcium transients were measured using the
310 Fluo-4 probe. LPC stimulation induced a significant increase in endothelial cell
311 Fluo4 signal (figure 5A), which was blocked by nifedipine and thapsigargin
312 (figure 5B). Moreover, EGTA, an extracellular Ca^{+2} chelator, and Bapta-AM, an
313 intracellular Ca^{+2} chelator, abrogated ROS generation induced by LPC
314 stimulation at 15 min (figure 5C).

315

316 **NOX5 knockdown attenuates LPC-induced inflammatory processes in** 317 **endothelial cells**

318 LPC increased monocyte adhesion to endothelial cells and increased
319 ICAM-1 expression. NOX5 knockdown decreased LPC-induced monocyte
320 adhesion to endothelial cells (figures 6A and 6B). ICAM-1 mRNA expression

321 was also attenuated in NOX5-silenced endothelial cells stimulated with LPC

322 (figure 6C).

323

324 **Discussion**

325 Oxidative stress is a critical player in endothelial dysfunction associated
326 with cardiovascular diseases. NOX enzymes play a major role in the
327 upregulated ROS production in atherosclerotic processes. However, the
328 mechanisms involved in NOXes activation are not entirely understood. Here,
329 we show that (1) LPC induces ROS production dependent on different NOX
330 isoforms at different time points; ROS production induced by LPC involves
331 NOX1/4 and NOX5 isotypes at late time points while NOX5 is important at early
332 time points; (2) LPC increases intracellular Ca^{2+} concentration and induces a
333 pro-inflammatory response in endothelial cells; (3) Calcium chelators prevent
334 LPC-induced endothelial ROS production; (4) NOX5 pharmacological inhibition
335 as well as NOX5 knockdown attenuates LPC-induced ROS generation and
336 endothelial cell activation.

337 LPC is an abundant component of oxidized low-density lipoprotein
338 (oxLDL) [30-33]. LPC activates apoptotic signaling [34, 35], induces vascular
339 dysfunction [32], promotes inflammatory cells infiltration of vascular walls [36],
340 and induces innate immune trans-differentiation of endothelial cells [12].
341 Upregulated ROS production contributes to the activation of signaling pathways
342 that result in endothelial injury. LPC-induced ROS generation has been
343 associated with NOX activation in HUVEC [37], leading to decrease NO
344 bioavailability and caspase-3 activation. However, the NOX isotype that
345 participates in this process was not identified.

346 LPC-induced ROS generation seems to be endothelial cell type-
347 dependent since Tsai et al. failed to observe this effect in cerebral bEND.3
348 endothelial cells [34]. Here, we found that LPC (10^{-5} M) induces ROS

349 production in a time-dependent manner in aortic endothelial cells (HAEC). This
350 pattern could be related to substrate availability for enzymatic ROS production,
351 such as the NADPH oxidase-dependent ROS production.

352 Guzik et al. [5] observed that arterial NOX5 protein expression is
353 increased in patients with coronary artery disease, contributing to increased
354 ROS production. As hyperlipidemia plays an important role in atherosclerosis-
355 related endothelial dysfunction, we used pharmacological inhibitors with
356 differential selectivity for the NOX isotypes to determine which NOX isotypes
357 contribute to LPC effect. In addition, different methodologies were used to
358 detect and confirm ROS production by LPC and to investigate the participation
359 of NOX5 in LPC-induced endothelial ROS production. Lucigenin and electron
360 paramagnetic spectroscopy showed NOX5-dependent ROS generation at early
361 time points for LPC stimulation. NOX5 knockdown decreased LPC-induced
362 ROS production, supporting data obtained in pharmacological assays.
363 Moreover, the continuous presence of LPC activated other NOX isotypes that,
364 along with NOX5, sustain ROS production, as demonstrated by decreased ROS
365 production in the presence of NOX1/4 dual inhibitor or selective NOX1 and
366 NOX5 inhibitors. These findings suggest that LPC induces NOX5 activity and
367 NOX5 inhibition attenuates or delays oxidative stress in hyperlipidemia
368 conditions, such as atherosclerosis.

369 Activation of different NOX isotypes under prolonged LPC stimulus may
370 be associated with ROS-induced ROS release [36, 37]. Sustained ROS
371 production can overwhelm the cellular ROS quenching capacity, leading to
372 redox unbalance, and oxidation of essential mitochondrial components (as
373 revised by Zorov DB. *et al* [38]) or of enzymes that modulate NOXes activity,

374 such as Src-family kinases [39] and others, like tyrosine phosphatases, whose
375 activity is inhibited by oxidation [40]. Inhibition of tyrosine phosphatase can also
376 increase ROS generation by disturbing tyrosine kinase signaling and organelles
377 function [19, 41]. Therefore, modulation of NOX5-dependent ROS generation,
378 as observed in the early stages of LPC stimulation, may prevent irreversibly
379 cellular damage related to ROS overproduction.

380 LPC incubation for longer period times (for 4 hours) did not change
381 NOX5 expression in endothelial cells (data not shown). However, LPC
382 increased intracellular Ca^{2+} concentration at time points where increased ROS
383 production was observed. Unlike other NOX isotypes, NOX5 activity relies on
384 Ca^{2+} influx [3, 5]. Despite of unchanged NOX5 protein expression, NOX5
385 activity was increased. Additionally, Ca^{2+} mobilization induced by LPC seems
386 to depend on both intra- and extracellular calcium stocks, since nifedipine, a
387 membrane calcium channel blocker, and thapsigargin, which perturbs and
388 reduces endoplasmic reticulum Ca^{2+} stock, prevented LPC-induced increased
389 intracellular Ca^{2+} concentrations. The calcium machinery is extremely complex
390 [42] and LPC perturbation of endothelial Ca^{2+} homeostasis demonstrates that it
391 may trigger many cellular mechanisms [12, 43], including activation of
392 NOX5, and, consequently, ROS production.

393 Finally, LPC has been shown to activate inflammatory signaling
394 pathways in endothelial cells [12], inducing cytokine production [44] and
395 upregulating adhesion molecules expression [45]. Here, we observed that
396 NOX5 knockdown attenuated LPC-induced ICAM-1 mRNA expression as well
397 as monocyte adhesion, important events in atherosclerosis development and
398 progression.

399 Together, these results suggest that control of NOX5 in pathological
400 conditions may improve endothelial function and attenuate inflammatory
401 responses to LPC.

402 In conclusion, our results demonstrate that NOX5-dependent ROS
403 production is essential to LPC-induced oxidative stress and inflammatory
404 response in endothelial cells. Moreover, our data suggest that NOX5
405 represents an important target to prevent endothelial cells activation and
406 atherosclerosis-associated oxidative and inflammatory processes.

407

408

409 **Legends to Figures**

410

411 **Figure 1 - LPC-induced ROS production in HAEC.** (A) ROS production after
412 short-time stimulations (5 min – 1 h). (B) ROS production after long-time
413 stimulations (4 h – 24 h). (C) Line graphic showing the profile of LPC-induced
414 ROS production, assessed by lucigenin assay. Data represent the mean \pm
415 SEM of n=5-8 experiments. One-way ANOVA followed by Tukey's multiple
416 comparisons test. * $p < 0.05$.

417

418 **Figure 2 - Role of NOX1 and NOX4 in LPC-induced ROS generation in**
419 **endothelial cells.** LPC stimulation for 15 min (A, C) and 4 h (B, D) in the
420 presence of vehicle or GKT137831 (10^{-5} M, NOX1/4 inhibitor) or noxa1ds (10^{-5}
421 M, NOX1 inhibitor). ROS generation was determined by Lucigenin assay. Data
422 represent the mean \pm SEM. One-way ANOVA followed by Tukey's multiple
423 comparisons test. * $p < 0.05$ and, ns= not significant.

424

425 **Figure 3 - Role of NOX5 in LPC-induced ROS generation in endothelial**
426 **cells.** ROS generation was measured by Lucigenin assay (A, B) and EPR
427 spectroscopy (C, D). LPC stimulation for 15 min (A, C) and 4 h (B, D) in the
428 presence of vehicle or Melittin (10^{-7} M, NOX5 inhibitor). Data represent the
429 mean \pm SEM of n= 4-10 experiments. One-way ANOVA followed by Tukey's
430 multiple comparisons test. * $p < 0.05$.

431

432

433

434 **Figure 4 – NOX5 knockdown abrogates LPC-induced ROS generation.**

435 ROS generation was measured by Lucigenin assay (A) in cells stimulated with
436 LPC (10^{-5} M) for 15 min. Endothelial NOX5 protein expression in control cells
437 (control), cells with negative control siRNA (mismatch) or siRNA for NOX5 (B).
438 Data represent the mean \pm SEM of n= 4-6 experiments. Two-way (A) or one-
439 way (B) ANOVA followed by Tukey's multiple comparisons test. * $p < 0.05$ and,
440 ns = not significant.

441

442 **Figure 5 – LPC-induced calcium mobilization in endothelial cells.** Relative

443 Fluo4 fluorescence signal during 30 min of LPC (10^{-5} M) stimulation (A). Area
444 under the curve (AUC) from data depicted in A (B). ROS generation was
445 measured by Lucigenin assay in cells stimulated with LPC (10^{-5} M) for 15 min in
446 the presence of Bapta-AM (10^{-6} M), EGTA (2×10^{-3} M) or Tiron (10^{-4} M) (C).
447 Data represent the mean \pm SEM of n= 5-7 experiments. One-way ANOVA
448 followed by Tukey's multiple comparisons test. * $p < 0.05$.

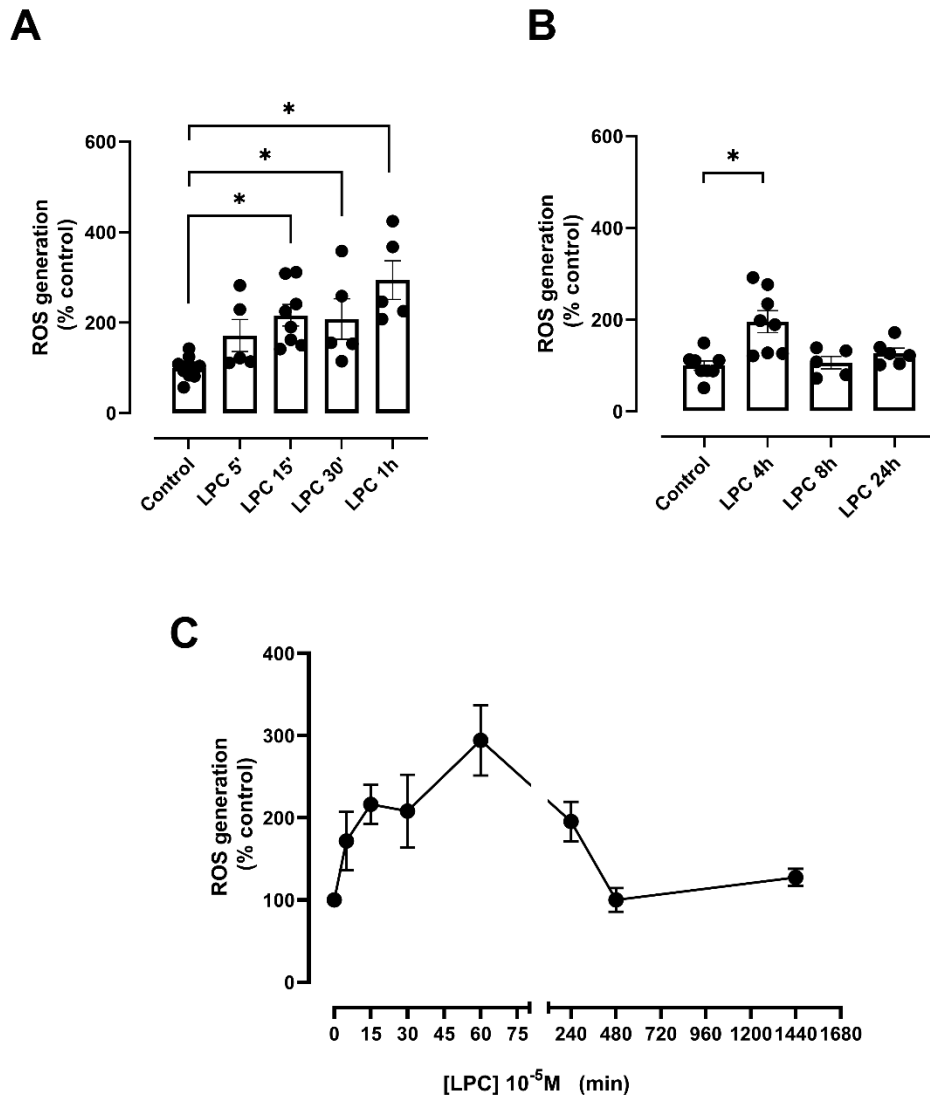
449

450 **Figure 6 – NOX5 knockdown attenuates endothelial cell activation.**

451 Photomicrography depicting labeled monocytes (CFSE probe, green) on LPC-
452 or vehicle-stimulated control endothelial cells (vehicle, lipofectamine),
453 endothelial cells submitted to NOX5 silencing (siRNA) or negative control siRNA
454 sequence (mismatch) (A). Fluorescence signals from labeled monocytes in A
455 (B). ICAM-1 mRNA expression (C). Data represent the mean \pm SEM of n= 5-8
456 experiments. Two-way ANOVA followed by Tukey's multiple comparisons test.
457 * $p < 0.05$.

458

459 **Figure 1**

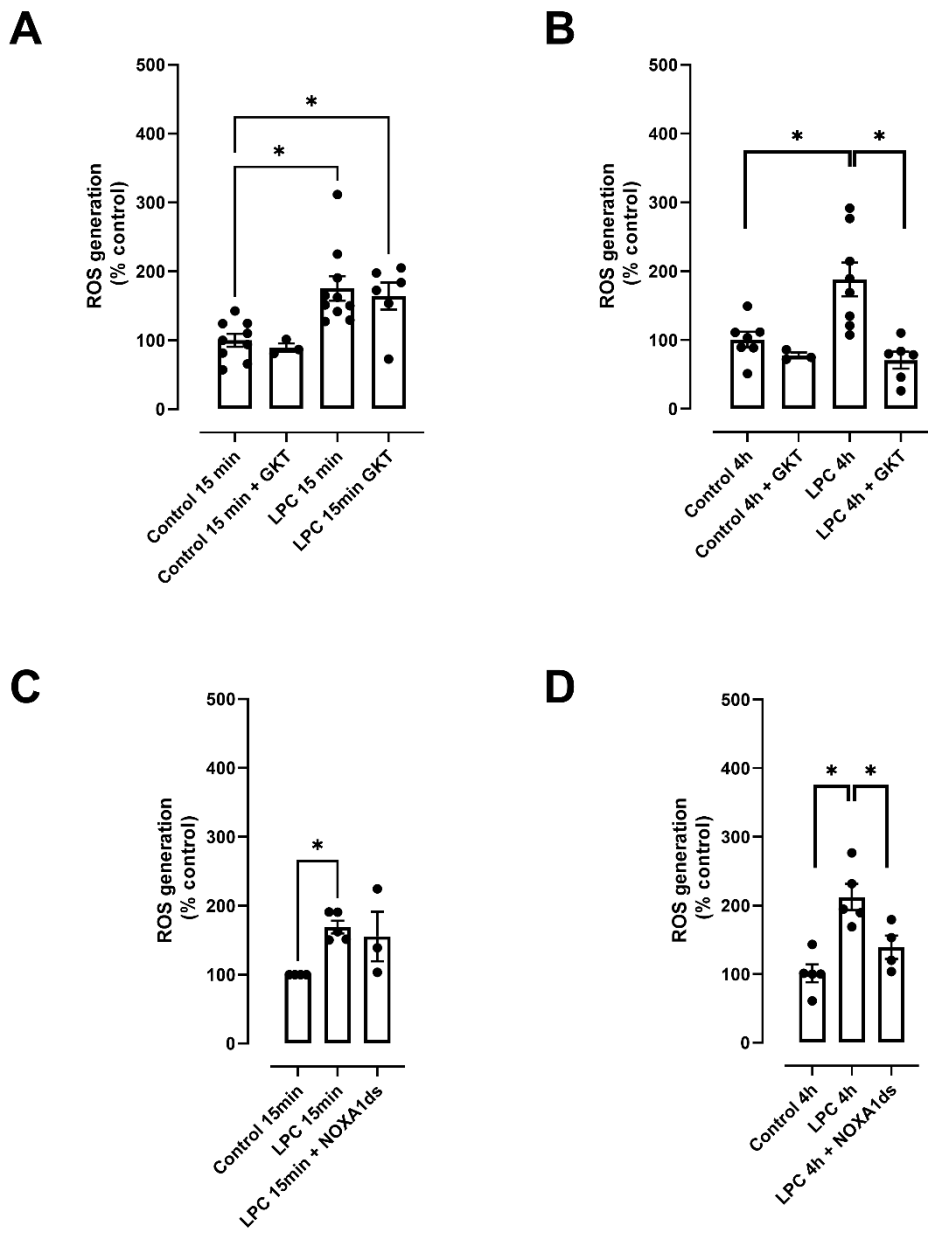


460

461

462 **Figure 2**

463

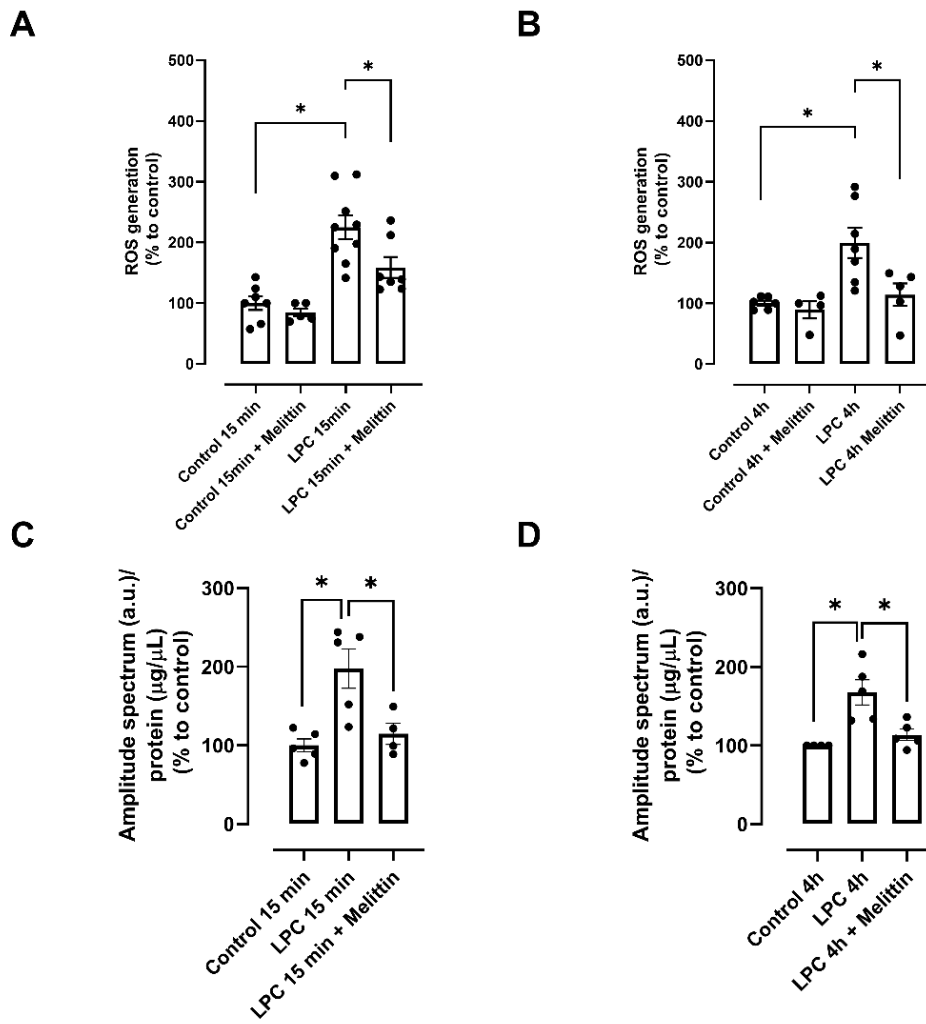


464

465

466 **Figure 3**

467



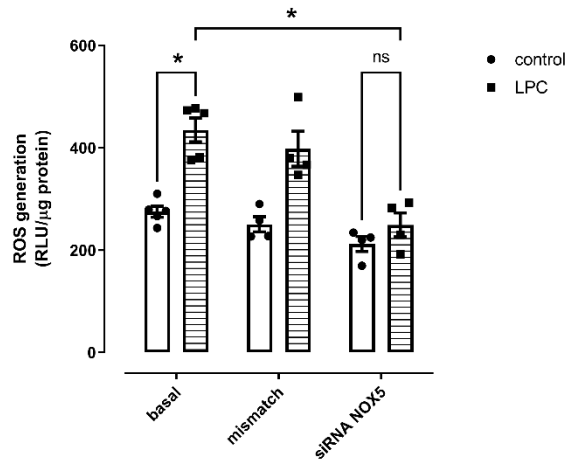
468

469

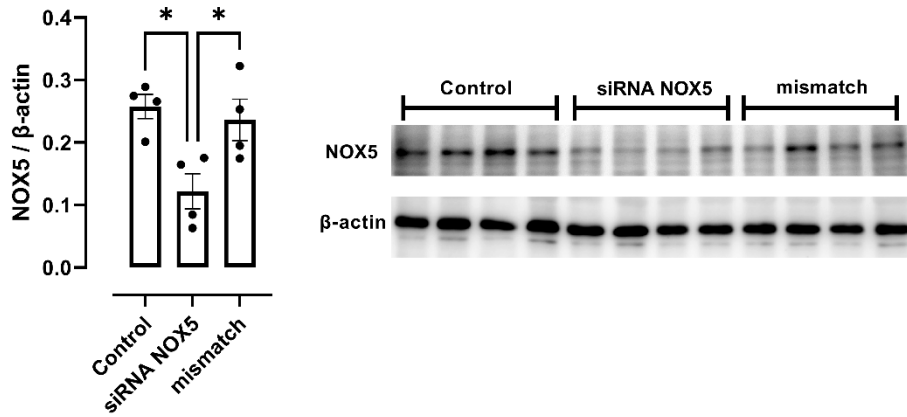
470 **Figure 4.**

471

A



B



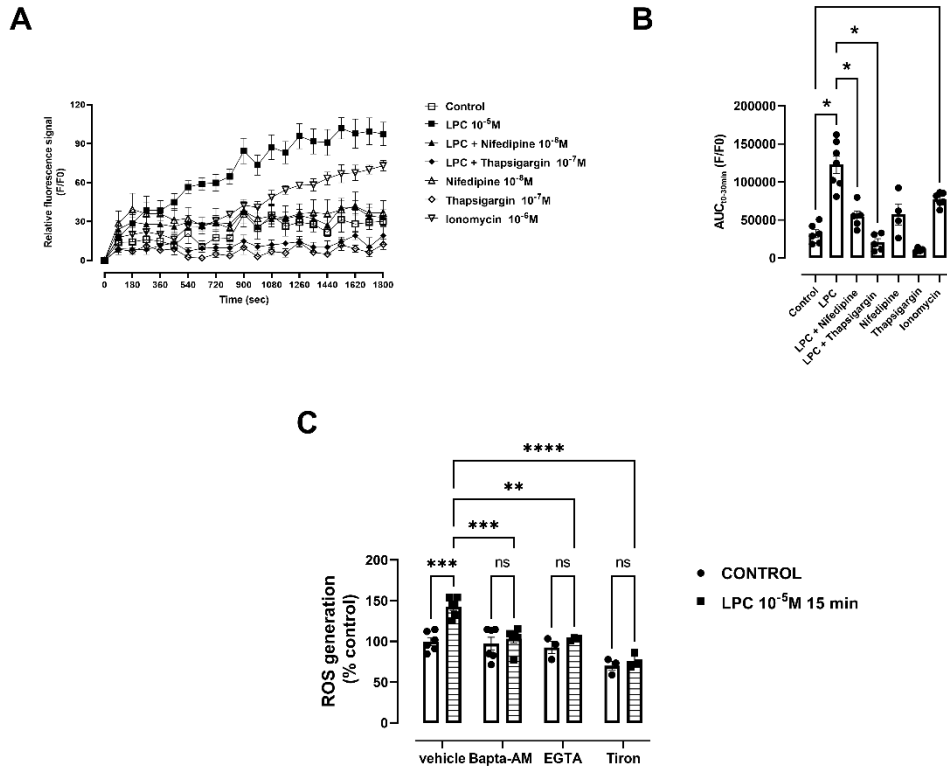
472

473

474 **Figure 5**

475

476



477

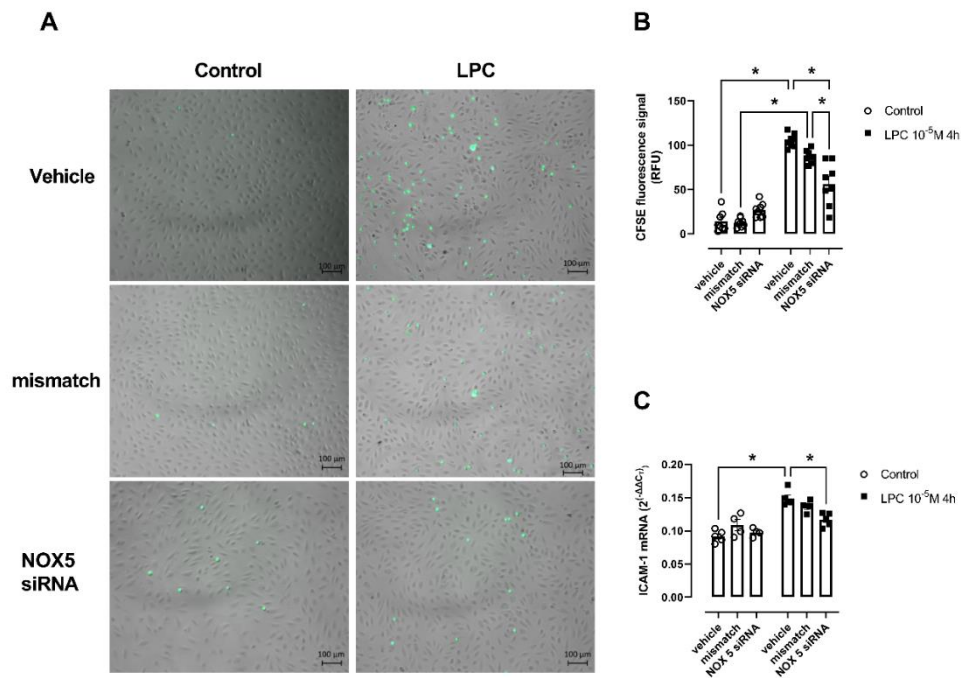
478

479

480

481 **Figure 6.**

482



483

484

485 **Acknowledgments**

486 This work was supported by grants from Fundação de Amparo à Pesquisa do
487 Estado de São Paulo (FAPESP-CRID 2013/08216-2; 2016/16207-1 to JFS),
488 Coordenação de Aperfeiçoamento de Pessoal de Nível Superior (CAPES) and
489 Conselho Nacional de Desenvolvimento Científico e Tecnológico (CNPq),
490 Brazil, to RCT.

491

492 **Conflict of Interest**

493 All authors declare no conflict of interest.

494

495 **Author Contributions**

496 All authors participated in the design of the study
497 JFS, JVA, JN, RMC - performed the experiments
498 RCT and RMT contributed with reagents or analytical tools
499 JFS - performed the data analysis
500 JFS and RCT wrote the paper
501 All authors discussed and critically reviewed the material

502

503 **Supplementary Material**

504 Supplementary Material is available on Arteriosclerosis, Thrombosis, and
505 Vascular Biology website. (ATVB 6.6) AHA

506

507 **References**

- 508 [1] - Yang X, Li Y, Li Y, et al. Oxidative Stress-Mediated Atherosclerosis: Mechanisms
509 and Therapies. *Front Physiol.* 2017; 8:600. Published 2017 Aug 23.
510 doi:10.3389/fphys.2017.00600.
- 511 [2] - Gimbrone MA Jr, García-Cardeña G. Endothelial Cell Dysfunction and the
512 Pathobiology of Atherosclerosis. *Circ Res.* 2016;118(4):620-636.
513 doi:10.1161/CIRCRESAHA.115.306301.
- 514 [3] - Touyz RM, Anagnostopoulou A, Rios F, Montezano AC, Camargo LL. NOX5:
515 Molecular biology and pathophysiology. *Exp Physiol.* 2019;104(5):605-616.
516 doi:10.1113/EP086204.
- 517 [4] – Montezano AC, Burger D, Paravicini TM, et al. Nicotinamide adenine dinucleotide
518 phosphate reduced oxidase 5 (Nox5) regulation by angiotensin II and endothelin-1 is
519 mediated via calcium/calmodulin-dependent, rac-1-independent pathways in human
520 endothelial cells. *Circ Res.* 2010;106(8):1363-1373.
521 doi:10.1161/CIRCRESAHA.109.216036.
- 522 [5] - Guzik TJ, Chen W, Gongora MC, et al. Calcium-dependent NOX5 nicotinamide
523 adenine dinucleotide phosphate oxidase contributes to vascular oxidative stress in
524 human coronary artery disease. *J Am Coll Cardiol.* 2008;52(22):1803-1809.
525 doi:10.1016/j.jacc.2008.07.063.
- 526 [6] - Law SH, Chan ML, Marathe GK, Parveen F, Chen CH, Ke LY. An Updated Review
527 of Lysophosphatidylcholine Metabolism in Human Diseases. *Int J Mol Sci.*
528 2019;20(5):1149. Published 2019 Mar 6. doi:10.3390/ijms20051149.
- 529 [7] - Li YF, Li RS, Samuel SB, et al. Lysophospholipids and their G protein-coupled
530 receptors in atherosclerosis. *Front Biosci (Landmark Ed).* 2016;21(1):70-88.
531 doi:10.2741/4377.

- 532 [8] - Chen L, Liang B, Froese DE, et al. Oxidative modification of low density lipoprotein
533 in normal and hyperlipidemic patients: effect of lysophosphatidylcholine composition on
534 vascular relaxation. *J Lipid Res.* 1997;38(3):546-553.
- 535 [9] - Zakiev ER, Sukhorukov VN, Melnichenko AA, Sobenin IA, Ivanova EA, Orekhov
536 AN. Lipid composition of circulating multiple-modified low density lipoprotein. *Lipids*
537 *Health Dis.* 2016;15(1):134. Published 2016 Aug 24. doi:10.1186/s12944-016-0308-2.
- 538 [10] - Kume N, Cybulsky MI, Gimbrone MA Jr. Lysophosphatidylcholine, a component
539 of atherogenic lipoproteins, induces mononuclear leukocyte adhesion molecules in
540 cultured human and rabbit arterial endothelial cells. *J Clin Invest.* 1992;90(3):1138-
541 1144. doi:10.1172/JCI115932.
- 542 [11] - Han MS, Lim YM, Quan W, et al. Lysophosphatidylcholine as an effector of fatty
543 acid-induced insulin resistance. *J Lipid Res.* 2011;52(6):1234-1246.
544 doi:10.1194/jlr.M014787.
- 545 [12] - Li X, Wang L, Fang P, et al. Lysophospholipids induce innate immune
546 transdifferentiation of endothelial cells, resulting in prolonged endothelial activation. *J*
547 *Biol Chem.* 2018;293(28):11033-11045. doi:10.1074/jbc.RA118.002752.
- 548 [13] - Diehl P, Nienaber F, Zaldivia MTK, et al. lysophosphatidylcholine is a Major
549 Component of Platelet Microvesicles Promoting Platelet Activation and Reporting
550 Atherosclerotic Plaque Instability. *Thromb Haemost.* 2019;119(8):1295-1310.
551 doi:10.1055/s-0039-1683409.
- 552 [14] - Meikle PJ, Wong G, Tsorotes D, et al. Plasma lipidomic analysis of stable and
553 unstable coronary artery disease. *Arterioscler Thromb Vasc Biol.* 2011;31(11):2723-
554 2732. doi:10.1161/ATVBAHA.111.234096
- 555 [15] - Ménégaut L, Masson D, Abello N, et al. Specific enrichment of 2-arachidonoyl-
556 lysophosphatidylcholine in carotid atheroma plaque from type 2 diabetic patients.
557 *Atherosclerosis.* 2016;251:339-347. doi:10.1016/j.atherosclerosis.2016.05.004

- 558 [16] – Li X, Fang P, Li Y, et al. Mitochondrial Reactive Oxygen Species Mediate
559 Lysophosphatidylcholine-Induced Endothelial Cell Activation. *Arterioscler Thromb Vasc*
560 *Biol.* 2016;36(6):1090-1100. doi:10.1161/ATVBAHA.115.306964.
- 561 [17] - Chaudhuri P, Rosenbaum MA, Sinharoy P, Damron DS, Birnbaumer L, Graham
562 LM. Membrane translocation of TRPC6 channels and endothelial migration are
563 regulated by calmodulin and PI3 kinase activation. *Proc Natl Acad Sci U S A.*
564 2016;113(8):2110-2115. doi:10.1073/pnas.1600371113.
- 565 [18] - da Costa RM, da Silva JF, Alves JV, et al. Increased O-GlcNAcylation of
566 Endothelial Nitric Oxide Synthase Compromises the Anti-contractile Properties of
567 Perivascular Adipose Tissue in Metabolic Syndrome. *Front Physiol.* 2018;9:341.
568 Published 2018 Apr 6. doi:10.3389/fphys.2018.00341.
- 569 [19] – Camargo LL, Harvey AP, Rios FJ, et al. Vascular Nox (NADPH Oxidase)
570 Compartmentalization, Protein Hyperoxidation, and Endoplasmic Reticulum Stress
571 Response in Hypertension. *Hypertension.* 2018;72(1):235-246.
572 doi:10.1161/HYPERTENSIONAHA.118.10824.
- 573 [20] - Bánfi B, Tirone F, Durussel I, et al. Mechanism of Ca²⁺ activation of the NADPH
574 oxidase 5 (NOX5). *J Biol Chem.* 2004;279(18):18583-18591.
575 doi:10.1074/jbc.M310268200.
- 576 [21] - Tostes RC, Wilde DW, Bendhack LM, Webb RC. The effects of cyclopiazonic
577 acid on intracellular Ca²⁺ in aortic smooth muscle cells from DOCA-hypertensive
578 rats. *Braz J Med Biol Res.* 1997;30(2):257-267. doi:10.1590/s0100-
579 879x1997000200016.
- 580 [22] - Ding WX, Ni HM, Gao W, et al. Differential effects of endoplasmic reticulum
581 stress-induced autophagy on cell survival. *J Biol Chem.* 2007;282(7):4702-4710.
582 doi:10.1074/jbc.M609267200.
- 583 [23] - Liu C, Hermann TE. Characterization of ionomycin as a calcium ionophore. *J Biol*
584 *Chem.* 1978;253(17):5892-5894.
- 585

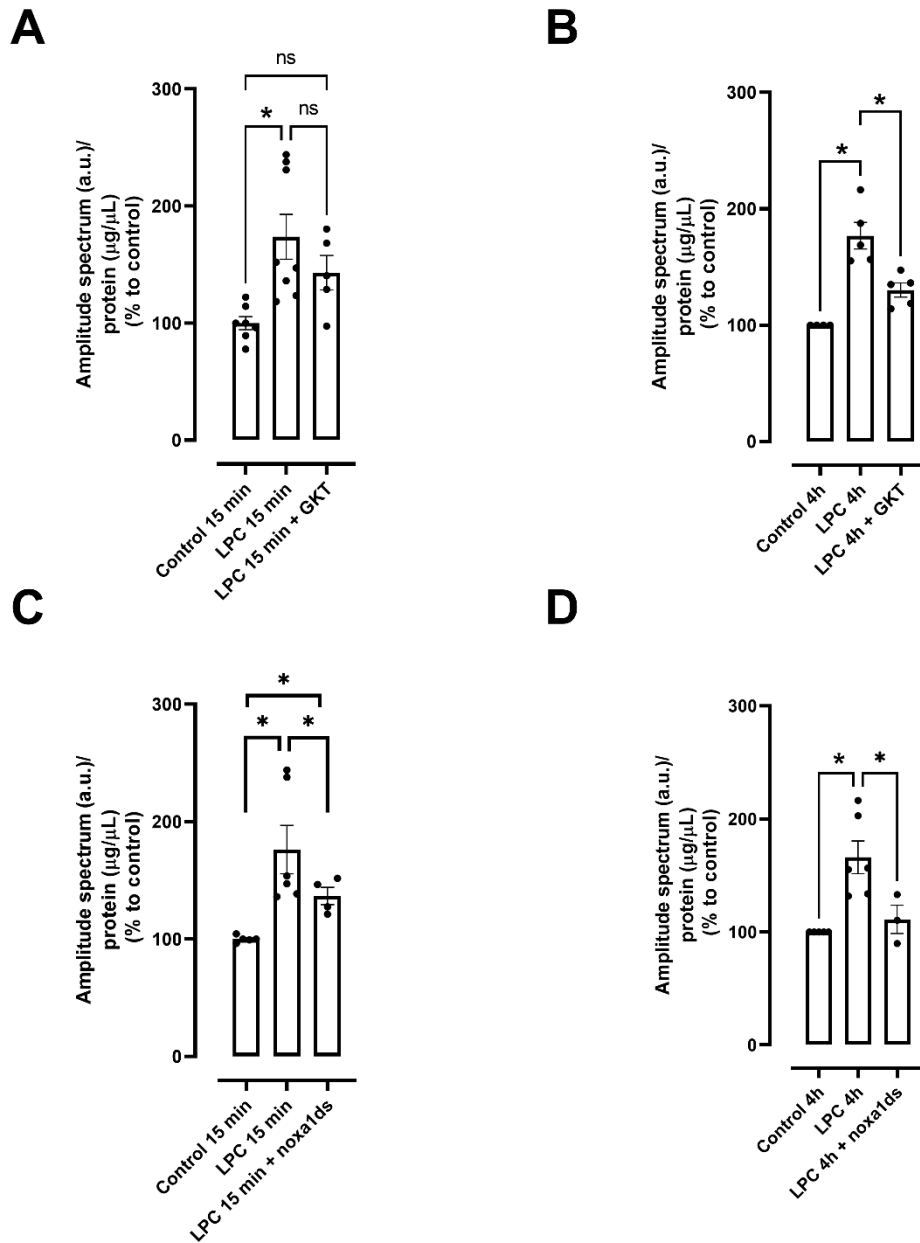
- 586 [24] - Kugelmann D, Rotkopf LT, Radeva MY, Garcia-Ponce A, Walter E, Waschke J.
587 Histamine causes endothelial barrier disruption via Ca²⁺-mediated RhoA activation
588 and tension at adherens junctions. *Sci Rep.* 2018;8(1):13229. Published 2018 Sep 5.
589 doi:10.1038/s41598-018-31408-3.
- 590 [25] - Giordano A, Romano S, D'Angelillo A, et al. Tirofiban counteracts endothelial cell
591 apoptosis through the VEGF/VEGFR2/pAkt axis. *Vascul Pharmacol.* 2016;80:67-74.
592 doi:10.1016/j.vph.2015.12.001.
- 593 [24] – Lopes RA, Neves KB, Pestana CR, et al. Testosterone induces apoptosis in
594 vascular smooth muscle cells via extrinsic apoptotic pathway with mitochondria-
595 generated reactive oxygen species involvement. *Am J Physiol Heart Circ Physiol.*
596 2014;306(11):H1485-H1494. doi:10.1152/ajpheart.00809.2013.
- 597 [25] - Dudley SC Jr, Hoch NE, McCann LA, et al. Atrial fibrillation increases production
598 of superoxide by the left atrium and left atrial appendage: role of the NADPH and
599 xanthine oxidases. *Circulation.* 2005;112(9):1266-1273.
600 doi:10.1161/CIRCULATIONAHA.105.538108.
- 601 [26] - Dikalov SI, Kirilyuk IA, Voinov M, Grigor'ev IA. EPR detection of cellular and
602 mitochondrial superoxide using cyclic hydroxylamines. *Free Radic Res.*
603 2011;45(4):417-430. doi:10.3109/10715762.2010.540242.
- 604 [27] - Neves KB, Nguyen Dinh Cat A, Lopes RA, et al. Chemerin Regulates Crosstalk
605 Between Adipocytes and Vascular Cells Through Nox. *Hypertension.* 2015;66(3):657-
606 666. doi:10.1161/HYPERTENSIONAHA.115.05616.
- 607 [28] - Dimitriadis GK, Kaur J, Adya R, et al. Chemerin induces endothelial cell
608 inflammation: activation of nuclear factor-kappa beta and monocyte-endothelial
609 adhesion. *Oncotarget.* 2018;9(24):16678-16690. Published 2018 Mar 30.
610 doi:10.18632/oncotarget.24659
- 611 [29] - Kugiyama K, Kerns SA, Morrisett JD, Roberts R, Henry PD. Impairment of
612 endothelium-dependent arterial relaxation by lysolecithin in modified low-density
613 lipoproteins. *Nature.* 1990;344(6262):160-162. doi:10.1038/344160a0

- 614 [30] – Hasegawa H, Lei J, Matsumoto T, Onishi S, Suemori K, Yasukawa M.
615 Lysophosphatidylcholine enhances the suppressive function of human naturally
616 occurring regulatory T cells through TGF- β production. *Biochem Biophys Res*
617 *Commun.* 2011;415(3):526-531. doi:10.1016/j.bbrc.2011.10.119
- 618 [31] - Chang MC, Lee JJ, Chen YJ, et al. lysophosphatidylcholine induces
619 cytotoxicity/apoptosis and IL-8 production of human endothelial cells: Related
620 mechanisms. *Oncotarget.* 2017;8(63):106177-106189. Published 2017 Nov 10.
621 doi:10.18632/oncotarget.22425.
- 622 [32] - Tsai TY, Leong IL, Cheng KS, et al. Lysophosphatidylcholine-induced cytotoxicity
623 and protection by heparin in mouse brain bEND.3 endothelial cells. *Fundam Clin*
624 *Pharmacol.* 2019;33(1):52-62. doi:10.1111/fcp.12399.
- 625 [33] - Park S, Kim JA, Choi S, Suh SH. Superoxide is a potential culprit of caspase-3
626 dependent endothelial cell death induced by lysophosphatidylcholine. *J Physiol*
627 *Pharmacol.* 2010;61(4):375-381.
- 628 [34] - Huang YH, Schäfer-Elinder L, Wu R, Claesson HE, Frostegård J.
629 Lysophosphatidylcholine (LPC) induces proinflammatory cytokines by a platelet-
630 activating factor (PAF) receptor-dependent mechanism. *Clin Exp Immunol.*
631 1999;116(2):326-331. doi:10.1046/j.1365-2249.1999.00871.x.
- 632 [35] - Heinloth A, Heermeier K, Raff U, Wanner C, Galle J. Stimulation of NADPH
633 oxidase by oxidized low-density lipoprotein induces proliferation of human vascular
634 endothelial cells. *J Am Soc Nephrol.* 2000;11(10):1819-1825.
- 635 [36] - Zorov DB, Juhaszova M, Sollott SJ. Mitochondrial reactive oxygen species (ROS)
636 and ROS-induced ROS release. *Physiol Rev.* 2014;94(3):909-950.
637 doi:10.1152/physrev.00026.2013.
- 638 [37] - Egea J, Fabregat I, Frapart YM, et al. European contribution to the study of ROS:
639 A summary of the findings and prospects for the future from the COST action BM1203
640 (EU-ROS) [published correction appears in *Redox Biol.* 2018 Apr;14 :694-696]. *Redox*
641 *Biol.* 2017;13:94-162. doi:10.1016/j.redox.2017.05.007.

- 642 [38] - Zorov DB, Juhaszova M, Sollott SJ. Mitochondrial reactive oxygen species (ROS)
643 and ROS-induced ROS release. *Physiol Rev.* 2014;94(3):909-950.
644 doi:10.1152/physrev.00026.2013.
- 645 [39] - Giannoni E, Taddei ML, Chiarugi P. Src redox regulation: again in the front line.
646 *Free Radic Biol Med.* 2010;49(4):516-527. doi:10.1016/j.freeradbiomed.2010.04.025.
- 647 [40] - Frijhoff J, Dagnell M, Godfrey R, Ostman A. Regulation of protein tyrosine
648 phosphatase oxidation in cell adhesion and migration. *Antioxid Redox Signal.*
649 2014;20(13):1994-2010. doi:10.1089/ars.2013.5643.
- 650 [41] - Chen K, Kirber MT, Xiao H, Yang Y, Keaney JF Jr. Regulation of ROS signal
651 transduction by NADPH oxidase 4 localization. *J Cell Biol.* 2008;181(7):1129-1139.
652 doi:10.1083/jcb.200709049.
- 653 [42] - Filippini A, D'Amore A, D'Alessio A. Calcium Mobilization in Endothelial Cell
654 Functions. *Int J Mol Sci.* 2019;20(18):4525. Published 2019 Sep 12.
655 doi:10.3390/ijms20184525.
- 656 [43] - Chaudhuri P, Colles SM, Damron DS, Graham LM. Lysophosphatidylcholine
657 inhibits endothelial cell migration by increasing intracellular calcium and activating
658 calpain. *Arterioscler Thromb Vasc Biol.* 2003;23(2):218-223.
659 doi:10.1161/01.atv.0000052673.77316.01.
- 660 [44] - Murugesan G, Sandhya Rani MR, Gerber CE, et al. lysophosphatidylcholine
661 regulates human microvascular endothelial cell expression of chemokines. *J Mol Cell*
662 *Cardiol.* 2003;35(11):1375-1384. doi:10.1016/j.yjmcc.2003.08.004.
- 663 [45] - Li X, Shao Y, Sha X, et al. IL-35 (Interleukin-35) Suppresses Endothelial Cell
664 Activation by Inhibiting Mitochondrial Reactive Oxygen Species-Mediated Site-Specific
665 Acetylation of H3K14 (Histone 3 Lysine 14). *Arterioscler Thromb Vasc Biol.*
666 2018;38(3):599-609. doi:10.1161/ATVBAHA.117.310626.
- 667
- 668

669 **Supplementary Material and Results**

670 **Supplementary figure 1**



671

672 **Supplementary Figure 1 - Role of NOX1 and NOX4 in LPC-induced**

673 **endothelial ROS generation, assessed by EPR spectroscopy. LPC**

674 stimulation for 15 min (A, C) and 4 h (B, D) was performed in the presence of

675 vehicle or GKT137831 (10^{-5} M, NOX1/4 inhibitor) or noxa1ds (10^{-5} M, NOX1

676 inhibitor). Data represent the mean \pm SEM of n= 3 – 8 experiments. One-way

677 ANOVA followed by Tukey's multiple comparisons test. * $p < 0.05$ and, ns= not
678 significant.